

## Section 2

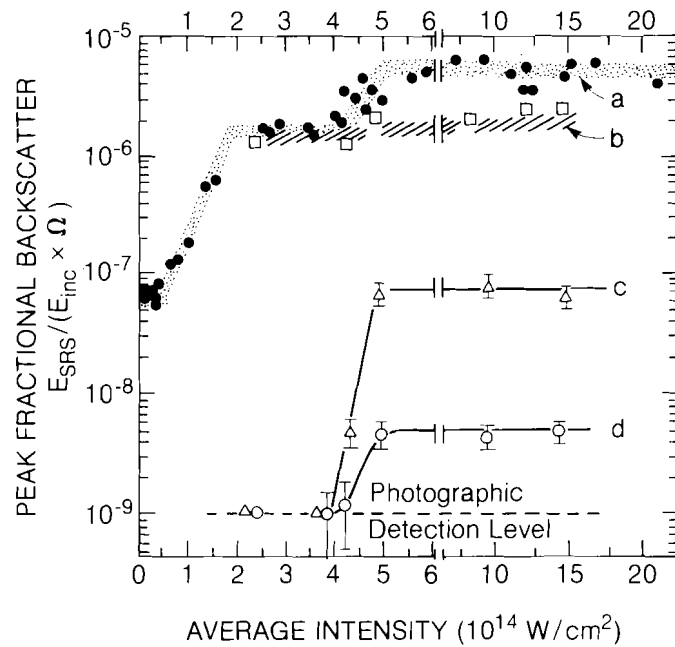
# PROGRESS IN LASER FUSION

### 2.A A New Model of Raman Spectra in Laser-Produced Plasma

Recent experiments have studied the spectral and temporal distribution of scattered light from planar and spherical laser-produced plasmas.<sup>1-4</sup> The reradiation at  $\omega_o/2$  (where  $\omega_o$  is the incident frequency) shows two relatively sharp increases when plotted as a function of increasing incident intensity.<sup>2</sup> These rises can be interpreted as the onset of the two-plasmon instability ( $2\omega_p$ ) and then the absolute stimulated Raman scattering (SRS-A), respectively, occurring near the quarter-critical ( $n_c/4$ ) surface in the plasma. Observation of a separated, broad band of radiation, lying in frequency between  $\omega_o$  and  $\omega_o/2$ , has been interpreted as evidence of the onset of the convective stimulated Raman instability (SRS-C) originating in the underdense region below  $n_c/4$ . The upper limit of this band corresponds to scattering from regions whose densities are as low as  $0.05 n_c$  and the lower part to regions with densities as large as  $0.2 n_c$ . Experimental observations of these two radiation features are shown in Figs. 19.1 and 19.2.<sup>2,4</sup>

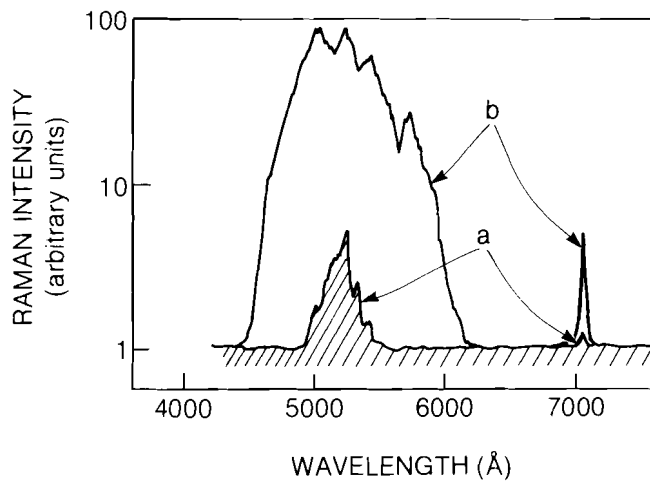
There have remained some difficulties in this SRS-C interpretation. One is the observation that the broadband radiation sets in at almost the same intensity as the SRS-A, despite the theoretical prediction that the convective threshold should be considerably higher if both instabilities occur in plasma with comparable density scale lengths. A second is the existence of the two gaps in the spectrum, one between the lower end of the band and  $\omega_o/2$ , and the other between the upper end and  $\omega_o$ . While the upper gap can be understood on

Fig. 19.1  
 Variation of the experimentally observed scattering with incident intensity. Curves "a" and "b" are the measured  $\omega_0/2$  components with polarization parallel and perpendicular, respectively, to the incident laser polarization. Curve "c" represents backscattering at 500 nm (between  $\omega_0/2$  and  $\omega_0$ ); curve "d" represents backscattering at  $\omega_0/2$ . The vertical axis for these last two curves is not absolutely calibrated.



P309

Fig. 19.2  
 Experimentally observed irradiation at  $\omega_0/2$  and in the  $\omega_0 - \omega_0/2$  band. Incident irradiation ( $\omega_0$ ) with 3510-Å laser-light threshold response is labeled "a." At higher incident intensities the response increases as in "b."



P319

the basis of Landau damping,<sup>4</sup> the lower gap requires invocation of density steepening near  $n_c/4$ .<sup>2</sup> This is despite the fact that the lower gap is always present in a variety of experimental situations, some of which show little evidence of steepening.

A third difficulty is that some limited observations<sup>5</sup> of the azimuthal angular distribution show little variation, while SRS-C calculations, using spatial gain from noise sources, incorporate angular terms in the exponential factors<sup>4</sup> and lead to the prediction of strong peaking out of the plane of polarization. Finally, a fourth problem is that spectrally and temporally resolved data<sup>2,4</sup> show that the scattering in the band region does not generally occur over large regions of frequency and/or time simultaneously. The effect is one of scintillation, suggesting contributions from localized regions during brief periods of time.

One approach to explain these difficulties has been to invoke the creation of filaments by self-focusing of hot spots of the incident light.<sup>3,4</sup> The greatly increased light intensity in the filament can exceed the threshold for SRS-C. The scintillation in time may be due to instability of the filaments themselves, while the spatial localization may be due to the existence of a density peak along the filament length.

In this note we propose an alternative explanation of the spectral band based on ordinary incoherent Thomson scattering. It is well known that incoherent scattering of radiation from plasma<sup>6</sup> exhibits a number of interesting features, including a Doppler-broadening characteristic of the ion temperature near the incident frequency  $\omega_0$ , and a sharp intense "plasma line" near the frequencies  $\omega_0 \pm \omega_p$  (Raman scattering). While the total scattered power in the plasma line is usually small compared with the incident power for a Maxwellian distribution of electrons, it can be much enhanced — as noted by Perkins and Salpeter.<sup>7</sup> In certain regions of the ionosphere, a two-temperature electron distribution is created in the daytime by absorption of the solar ultraviolet and x-rays, producing energetic photoelectrons in the 1- to 30-eV range while the bulk distribution has a temperature of only about 0.2 eV. This velocity distribution can result in increases in the plasma line intensity by factors of 50 to 100.

Even more enhancement may occur in the underdense corona of a laser-irradiated target. In this case, the sources of hot electrons are the  $2\omega_p$  and SRS-A instabilities occurring near the  $n_c/4$  surface. The hot-electron pulses resulting from the intermittent breaking of plasma waves near  $n_c/4$  move out into the corona and produce a transient local velocity distribution which can be modeled as a Maxwellian with temperature  $T_c$  for the bulk of the electrons, together with a narrow moving pulse of hot electrons moving in the radial direction.

The resultant scattered intensity is evaluated by integrating over the plasma volume, in much the same way as it is done in Ref. 7. The principal contribution to the integral is from the appropriate plasma line. The expression for the fractional scattered power has the usual Thomson scattering angular variation and the usual magnitude, multiplied by a shape factor  $S$  which is

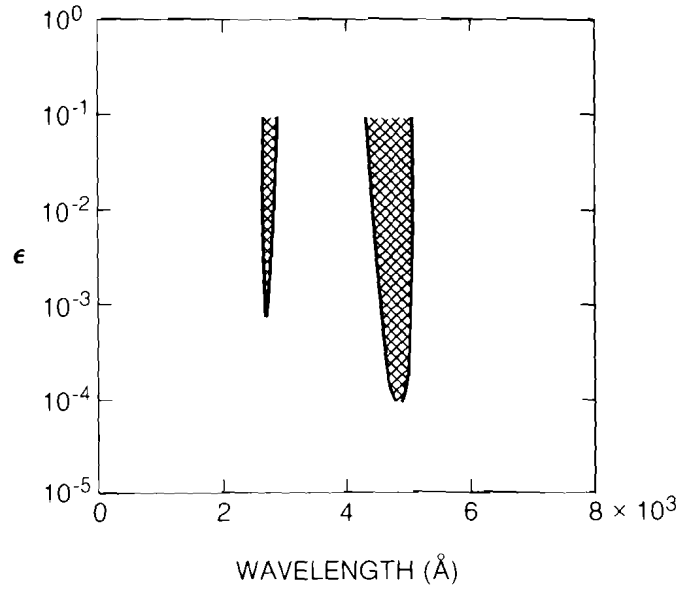
$$S = \frac{\left(\frac{E_p}{T_c}\right)^{1/2} \exp(-E_p/T_c) + \frac{T_c}{E_p} \frac{\bar{\nu}}{\omega}}{\frac{\bar{\nu}}{\omega} + \left(\frac{E_p}{T_c}\right)^{3/2} \exp(-E_p/T_c) + \epsilon \alpha^{3/2} y^2 (y-1) \exp[-\alpha(y-1)^2]} \quad (1)$$

Here  $E_p \equiv \frac{1}{2}m(\omega/k)^2$ ,  $\omega = \omega_0 - \omega_s$ ,  $k = |\mathbf{k}_0 - \mathbf{k}_s|$ , with  $\omega_s$  and  $\mathbf{k}_s$  the frequency and wave vector of the scattered EM wave. The electron collision frequency is denoted by  $\bar{\nu}$  and the ratio of the hot-electron density to the cold-electron density by  $\epsilon$  (assumed small). Also  $\alpha = 3T_h/2T_c$  and  $y^2 = 2E_p k^2 / (3k_r T_h)$  with  $T_h$  representing the equivalent temperature associated with the central velocity  $v_h$  of the moving electron pulse,  $3T_h = mv_h^2$ ;  $k_r$  is the radial component of  $\mathbf{k}$ . Equation (1) is not valid for  $\omega_s = \omega_0$  since it has been assumed that  $\omega/k \gg (2T_c/m)^{1/2}$ .

Major enhancement of the reflected power can occur for  $\omega_s$  and  $k_s$  such that the corresponding radial component of the plasma-wave phase velocity,  $\omega/k_r$ , falls on the increasing slope portion of the hot-electron pulse, i.e.,  $y < 1$ . If  $\epsilon$  is large enough, the denominator in Eq. (1) will then become small or negative. The homogeneous-dressed test-particle model is invalid in this limit, but it is certain that very large enhancements will occur. A proper calculation of the scattered intensity will require the solution of a nonlinear problem.

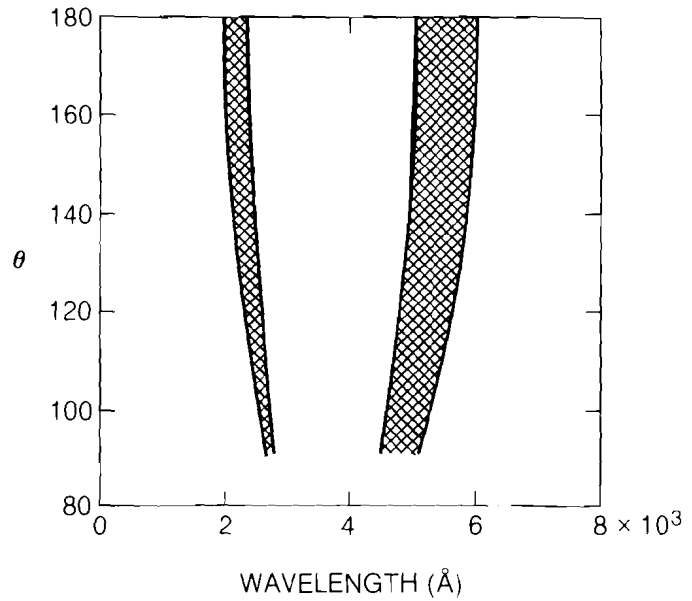
One finds that the two gaps in the spectrum occur in a natural way once  $\epsilon$  exceeds this critical level. For  $\omega_s$  near  $\omega_0/2$ , the plasma-wave phase velocity is high, the resistive terms dominate in Eq. (1) and  $S = O(10^{-2})$  for parameters appropriate to the experiments described in Ref. 2 ( $T_c = 1$  keV). The resultant scattered intensity is below the experimental detection level by a factor of  $10^2$ – $10^3$ . Again, when  $\omega_s$  approaches  $\omega_0$  [but not so close that Eq. (1) is invalid], the phase velocity becomes small enough that the Landau-damping term of the cold electrons dominates and again  $S = O(10^{-2})$ . These same considerations predict a separated band in the "up-scattering" regions between  $\omega_0$  and  $2\omega_0$  (but not symmetrical to the lower one since  $k_s$  will be larger).

If one defines the enhanced radiation intervals as corresponding to regions where the denominator of Eq. (1) vanishes or is negative, it is easy to explore the dependence on various parameters. Using a computer, we have studied the variation of the bands with  $\epsilon$ ,  $T_c$ ,  $T_h$ , and scattering angle  $\theta$ . An example of these results is shown in Figs. 19.3 and 19.4. In Fig. 19.3, the beginning of "down-scattering" is seen when  $\epsilon$  exceeds  $10^{-4}$ . The up-scattering sets in when  $\epsilon$  exceeds  $10^{-3}$ . These results are for  $T_c = 1$  keV,  $T_h = 18$  keV, and for an internal scattering angle of  $90^\circ$ . Note the broadening of the bands as  $\epsilon$  increases. Figure 19.4 illustrates shifting and broadening of the bands as the internal scattering angle is varied, for  $T_c = 1$  keV,  $T_h = 18$  keV, and  $\epsilon = 5 \times 10^{-3}$ . We have also noted smaller shifting with variation of  $T_h$ , and relatively little with variation of  $T_c$ . Recent experimental observations<sup>8</sup> have observed the up-scattered band as well as the down-scattered band, close to where these calculations predict them to be.



P288

Fig. 19.3  
 Variation of enhanced Raman-scattering band (hatched area) with  $\epsilon$ , the ratio of hot-electron density to cold-electron density. This is for scattering at an (internal) angle of  $90^\circ$  with  $T_h = 18 \text{ keV}$ ,  $T_c = 1.0 \text{ keV}$ , and incident wavelength  $\lambda_0 = 3510 \text{\AA}$ .



P287

Fig. 19.4  
 Variation of enhanced Raman-scattering band (hatched area) with (internal) angle of scattering. This is for  $\epsilon = 5 \times 10^{-3}$ , where  $\epsilon$  is the ratio of hot-electron to cold-electron density.  $T_h = 18 \text{ keV}$ ,  $T_c = 1.0 \text{ keV}$ , and incident wavelength  $\lambda_0 = 3510 \text{\AA}$ .

Our model also accounts for the other features discussed earlier. The coupling between the onset of the Raman spectrum and the onset of SRS-A is clear since it is presumably the hot electrons from the SRS-A at  $n_c/4$  which establish the reversed-slope plasma medium in the subcritical region (i.e., raise the value of  $\epsilon$  to the critical point). The scintillation clearly arises from the turbulent-pulsed nature of this same source. The azimuthal angular distribution of this ordinary Thomson scattering is relatively gentle compared to the SRS-C. Even at  $90^\circ$ , it is simply  $\sin^2\theta$ .

In summary, we propose a new model of the Raman spectra observed in laser experiments in inhomogeneous plasma. The scattering is due to ordinary incoherent Thomson scattering (using a greatly enhanced plasma line). The wakes of the incoherent "dressed" electrons are enlarged owing to a reversed-slope velocity distribution in the subcritical region created by bursts of hot electrons moving out from the quarter-critical surface and created there by the breaking of waves resulting from the SRS-A or  $2\omega_p$  instabilities. A unique feature of the model is the prediction of appreciable up-scattering, the existence of which has been experimentally observed.

#### ACKNOWLEDGMENT

This work was supported by the U.S. Department of Energy Office of Inertial Fusion under contract number DE-AC08-80DP40124 and by the Laser Fusion Feasibility Project at the Laboratory for Laser Energetics which has the following sponsors: Empire State Electric Energy Research Corporation, General Electric Company, New York State Energy Research and Development Authority, Northeast Utilities Service Company, Southern California Edison Company, The Standard Oil Company, and University of Rochester. Such support does not imply endorsement of the content by any of the above parties.

#### REFERENCES

1. D. W. Phillion *et al.*, *Phys. Fluids* **25**, 1434 (1982).
2. K. Tanaka, L. M. Goldman, W. Seka, M. C. Richardson, J. M. Soures, and E. A. Williams, *Phys. Rev. Lett.* **48**, 1179 (1982).
3. R. E. Turner, D. W. Phillion, E. M. Campbell, and K. G. Estabrook, *Phys. Fluids* **26**, 579 (1983).
4. W. Seka, E. A. Williams, R. S. Craxton, L. M. Goldman, R. W. Short, and K. Tanaka, submitted to *Phys. Fluids*.
5. W. Seka (private communication).
6. E. E. Salpeter, *Phys. Rev.* **120**, 1528 (1960).
7. F. Perkins and E. E. Salpeter, *Phys. Rev.* **139**, A55 (1965).
8. L. M. Goldman, W. Seka, K. Tanaka, A. Simon, and R. Short, presented at 14th Annual Anomalous Absorption Conference, Charlottesville, VA, 1984 (unpublished).